




## Article

# Maslinic Acid Supplementation during the In Vitro Culture Period Ameliorates Early Embryonic Development of Porcine Embryos by Regulating Oxidative Stress

Ting-Ting Yang <sup>†</sup>, Jia-Jia Qi <sup>†</sup>, Bo-Xing Sun <sup>†</sup>, He-Xuan Qu, Hua-Kai Wei, Hao Sun, Hao Jiang , Jia-Bao Zhang  and Shuang Liang <sup>\*</sup> 

Department of Animals Sciences, College of Animal Sciences, Jilin University, Changchun 130062, China

<sup>\*</sup> Correspondence: liangshuang85@jlu.edu.cn

<sup>†</sup> These authors are contributed equally to this work.

**Simple Summary:** High-quality early embryos are essential for accelerating animal reproduction and genetic modification of mammals, and oxidative stress is strongly associated with a decline in *in vitro* embryo developmental potential. During *in vitro* culture, the most direct and effective approach to alleviate oxidative stress is to add antioxidants to the *in vitro* culture medium. In this study, maslinic acid (MA), a pentacyclic triterpenoid acid in olive plants possessing antioxidant capacities due to its ability to scavenge free radicals, ameliorated the *in vitro* developmental capability of porcine embryos from parthenogenetic activation and somatic cell nuclear transfer. MA also enhanced oxidation resistance, maintained mitochondrial function, and inhibited apoptosis in porcine early-stage embryos.

**Abstract:** As a pentacyclic triterpene, MA exhibits effective free radical scavenging capabilities. The purpose of this study was to explore the effects of MA on porcine early-stage embryonic development, oxidation resistance and mitochondrial function. Our results showed that 1  $\mu$ M was the optimal concentration of MA, which resulted in dramatically increased blastocyst formation rates and improvement of blastocyst quality of *in vitro*-derived embryos from parthenogenetic activation (PA) and somatic cell nuclear transfer (SCNT). Further analysis indicated that MA supplementation not only significantly decreased the abundance of intracellular reactive oxygen species (ROS) and dramatically increased the abundance of intracellular reductive glutathione (GSH) in porcine early-stage embryos, but also clearly attenuated mitochondrial dysfunction and inhibited apoptosis. Moreover, Western blotting showed that MA supplementation upregulated OCT4 ( $p < 0.01$ ), SOD1 ( $p < 0.0001$ ) and CAT ( $p < 0.05$ ) protein expression in porcine early-stage embryos. Collectively, our data reveal that MA supplementation exerts helpful effects on porcine early embryo development competence via regulation of oxidative stress (OS) and amelioration of mitochondrial function and that MA may be useful for increasing the *in vitro* production (IVP) efficiency of porcine early-stage embryos.

**Keywords:** maslinic acid; porcine early embryos; oxidation resistance; mitochondrial function



**Citation:** Yang, T.-T.; Qi, J.-J.; Sun, B.-X.; Qu, H.-X.; Wei, H.-K.; Sun, H.; Jiang, H.; Zhang, J.-B.; Liang, S. Maslinic Acid Supplementation during the In Vitro Culture Period Ameliorates Early Embryonic Development of Porcine Embryos by Regulating Oxidative Stress. *Animals* **2023**, *13*, 1041. <https://doi.org/10.3390/ani13061041>

Academic Editors: Ramanathan K. Kasimanickam and John P. Kastelic

Received: 13 February 2023

Revised: 3 March 2023

Accepted: 5 March 2023

Published: 13 March 2023



**Copyright:** © 2023 by the authors. Licensee MDPI, Basel, Switzerland. This article is an open access article distributed under the terms and conditions of the Creative Commons Attribution (CC BY) license (<https://creativecommons.org/licenses/by/4.0/>).

## 1. Introduction

Compared with *in vivo*-derived embryo collection, IVP of porcine early-stage embryos is a highly essential technique that supplies sufficient quantities of embryos for biotechnology applications such as cloning [1] and genetic modification [2]. Thus, the IVP of high-implantation-potential embryos is an essential step in the process of creating porcine models for biomedical research.

Embryo *in vitro* culture (IVC), a crucial part of the IVP procedure, is a complex system that mimics *in vivo* conditions [3,4]. During IVC, embryos are cultured in controlled laboratory settings with a synthetic medium. Despite substantial progress in the field of

IVC optimization, *in vitro*-derived embryos have a lower ratio of early-stage development than *in vivo*-cultured embryos [5]. Long-term accumulation of ROS within embryos during the process of IVC has been established as a significant factor altering *in vitro* embryo quality [6]. Importantly, OS caused by an imbalance between antioxidants and ROS can negatively affect the efficiency of IVC [7]. Excessive ROS exert their pathological effects through damage to cellular organelles [8] and alterations in enzymatic function [9]. Compared with embryos of other species, porcine embryos contain large amounts of stored lipids; therefore, they are more sensitive to environmental conditions in IVC [10]. At present, antioxidant supplementation in the embryo IVC medium is an effective approach to overcome embryonic OS. Various antioxidants, such as resveratrol [11], melatonin [12,13], vitamin C [14], laminarin [15] and asiatic acid [16], have been widely used to alleviate OS by interrupting free-radical chain reactions. However, an optimized system for the effective mitigation of OS-induced embryo damage still needs to be developed.

MA (2 $\alpha$ ,3 $\beta$ -2,3-dihydroxyolean-12-en-28-oic acid), a plant secondary metabolite, is a triterpenoid compound principally obtained from olive tree (*Olea europaea* L.) [17]; however, it can also be extracted from *Lamprothyrus hieronymi* Schum. [18], *Tetracentron sinense* Oliv. [19] and *Geum japonicum* [20]. MA and its derivatives exert many beneficial pharmacological effects on cells, such as anticancer [21,22], antidiabetic [23], antiviral [24], antimicrobial [25], anti-inflammatory [26–28] and antiplatelet aggregation [29] activities. Extensive studies have suggested that MA can scavenge free radicals as a natural antioxidant [30–34]. Previously, it has been shown that the Akt/Nrf2/HO-1 pathway is involved in the antioxidative activity of MA to vascular smooth muscle cells (VSMCs) [35]. Furthermore, MA-treated diabetic animals have been shown to have reduced malondialdehyde levels, which increases the activity of glutathione peroxidase (GPX) and superoxide dismutase (SOD) in renal, cardiac, and hepatic tissues [36].

Although extensive experiments have shown that MA has a strong ability to scavenge free radicals and relieves oxidative damage to cells or tissues *in vivo* and *in vitro*, the influence of MA on porcine early-stage embryos is rarely reported. Thus, we hypothesized that supplementation with the natural antioxidant MA would be able to relieve systemic OS in porcine early-stage embryos *in vitro*, thereby helping to improve developmental competence. This study first investigated the effects of MA supplementation on the developmental competence of porcine *in vitro*-cultured embryos derived from PA and SCNT. Subsequently, we further analysed the mechanism underlying the promotion of MA on developmental competence of porcine early-stage embryos.

## 2. Materials and Methods

All chemical reagents involved in the study were purchased from Sigma-Aldrich (St. Louis, MO, USA) unless otherwise specified.

### 2.1. Porcine Oocyte Collection and In Vitro Maturation (IVM)

Porcine ovary collection was carried out at a local abattoir within 2 h of obtaining the prepubertal gilts, then delivered to the laboratory in 0.9% saline at 35–37 °C. Cumulus–oocyte complexes (COCs) were collected using a 10 mL syringe aspirating method. According to the IETS grading system, COCs of grade B and above were selected under a stereomicroscope (S22-LGB, Nikon, Shanghai, China), transferred to maturation medium [37] and incubated for 42–44 h at 38.5 °C under 5% CO<sub>2</sub> in 100% humidified air with mineral oil in 4-well plates (144444, Thermo Fisher, Shanghai, China). Fifty to sixty COCs were cultured in 500  $\mu$ L of maturation medium per well.

After IVM, the COCs were digested with 0.1% hyaluronidase to remove the surrounding expanded cumulus corona cell. Only the oocytes with homogeneous ooplasm and a polar body were subjected to subsequent experiments.

## 2.2. PA, SCNT and IVC

PA and SCNT procedures were performed according to our previous study [38]. After completing PA and SCNT, approximately 50 activated or reconstructed embryos were transferred to 500  $\mu$ L porcine IVC medium with mineral oil and continuously cultured in 4-well plates at 38.5 °C, 5% CO<sub>2</sub> and saturated humidity without changing the medium for 7 days. The day on which the activated or reconstructed embryos were transferred to the IVC medium was denoted as day 0. In this experiment, the percentages of 2-cell and 4-cell embryos, formed blastocysts and hatched blastocysts to the total number of embryos observed on day 2, day 6 and day 7 were counted as cleavage rate, blastocyst formation rate, and hatching rate, respectively.

MA was added to the IVC medium at a final concentration of 1  $\mu$ M, 2  $\mu$ M or 5  $\mu$ M.

## 2.3. Total Cell Number Assay in Blastocysts

To count the total cell numbers in blastocysts, day 6 porcine blastocysts were fixed in 4% paraformaldehyde (*w/v*) at room temperature for 30 min. Subsequently, the blastocysts were stained with 10  $\mu$ g/mL Hoechst 33342 for 10 min. Then, the stained embryos were mounted on glass slides, covered with cover slips and observed under a fluorescence microscope (Axio Vert.A1, Zeiss, Germany). The fluorescence signal intensities in each group of embryos were analysed with ImageJ software (National Institutes of Health, Bethesda, MD, USA).

## 2.4. 5-Ethynyl-2'-Deoxyuridine (EDU) Analysis

The cell proliferation of porcine blastocysts was detected using BeyoClick™ EDU with an Alexa Fluor 555 cell proliferation kit (C0075S, Beyotime, Shanghai, China) as specified in the manufacturer's protocols. Briefly, blastocysts were incubated with 10  $\mu$ M EDU at 38.5 °C and 5% CO<sub>2</sub> in air with saturated humidity for 2 h in the dark. At the end of incubation, the blastocysts were washed with PBS-PVA three times and fixed with 4% paraformaldehyde for 15 min. Then, the blastocysts were permeabilized by treatment with 0.1% Triton X-100 for 10 min and then washed with PBS-PVA three times. Next, the blastocysts were stained with Azide 555 solution for 30 min and 10  $\mu$ g/mL Hoechst 33342 for 8 min in the dark. After washing with PBS-PVA three times, the blastocysts were mounted on glass slides and observed under a fluorescence microscope. The EDU-positive cells were analysed with NIH ImageJ software.

## 2.5. TUNEL Assay in Blastocysts

In brief, porcine blastocysts were fixed in 4% paraformaldehyde for 1 h. Next, the blastocysts were permeabilized with 0.1% Triton X-100 for 10 min. The blastocysts were washed with PBS-PVA three times and incubated in the dark for 1 h at 37 °C with TUNEL detection solution (MA0223, Dalian Meilun Biotechnology, Dalian, China). Subsequently, the blastocysts were stained with 10  $\mu$ g/mL Hoechst 33342 for 15 min in the dark. The blastocysts were mounted on glass slides after washing three times and detected under a fluorescence microscope. The apoptotic nuclei in blastocysts were analysed with NIH ImageJ software.

## 2.6. Intracellular ROS and GSH Abundance Analysis

To determine intracellular ROS abundance, porcine 4-cell- or blastocyst-stage embryos were incubated with 10  $\mu$ M 2',7'-dichlorodihydrofluorescein diacetate (DCFH-DA; S0033S, Beyotime, Shanghai, China) for 15 min. Furthermore, porcine embryos were cultured in IVC medium with or without 1  $\mu$ M MA for 2 or 6 days under oxidative damage conditions (200  $\mu$ M H<sub>2</sub>O<sub>2</sub> preincubation for 30 min) to define whether MA reversed the oxidative damage in porcine embryos. To determine intracellular GSH levels, porcine 4-cell- or blastocyst-stage embryos were incubated with 10  $\mu$ M 4-chloromethyl-6,8-difluoro-7-hydroxycoumarin (CMF2HC; C12881, Thermo Fisher, Shanghai, China) for 30 min. The fluorescence signals of both ROS and GSH were captured in tagged image file format

(TIFF) using a digital camera connected to the fluorescence microscope, and fluorescence intensities were analysed using NIH ImageJ software.

### 2.7. Western Blot Assay

For Western blotting, embryos in each group ( $n = 80$ /per replicate) were collected and roundly lysed in lysis buffer comprising 40% ddH<sub>2</sub>O, 0.5 mM Tris-HCl, 50% glycerol, 10% SDS, bromophenol blue and  $\beta$ -mercaptoethanol at 95 °C. Next, the protein samples were resolved using 12% SDS-polyacrylamide gel electrophoresis (SDS-PAGE), and then transferred to polyvinylidene fluoride (PVDF) membranes. The PVDF membranes were sealed using 5% BSA at room temperature for 2 h; incubated overnight at 4 °C with primary antibodies against OCT4 (1:800, WL03686, Wanleibio, Shenyang, China); CAT (1:4000, 66765-1-Ig, Proteintech, Wuhan, China), SOD1 (1:2000, 10269-1-AP, Proteintech) and GAPDH (1:10,000, 60004-1-Ig, Proteintech); and then incubated with an HRP-conjugated anti-rabbit secondary antibody (1:10,000, SA00001-2, Proteintech) or anti-mouse secondary antibody (1:8000, SA00001-1, Proteintech) for 1.5 h. After washing with 1x TBST three times, the immunoblots were visualized with ECL solution (SQ201, Epizyme, Shanghai, China) by using a Tanon 5200 Image Analyser (Tanon, Shanghai, China) and analysed with NIH ImageJ software.

### 2.8. Reverse Transcription Quantitative Polymerase Chain Reaction (RT-qPCR) Analysis

Day-6 embryos in each group ( $n = 60$ /per replicate) were extracted for total RNA using TRIzol Reagent (Takara, Japan). The total RNA was reverse transcribed into cDNA (200 ng) with a Prime Script™ RT Reagent Kit (Takara, Japan). RT-qPCR was performed using SYBR Green Real-Time PCR Master Mix (Roche, Basel, Switzerland) in a PCRmax (Eco, Staffordshire, UK). RT-qPCR was performed in a 10  $\mu$ L reaction with 5  $\mu$ L of SYBR Green Real-Time PCR Master Mix, 2  $\mu$ L of ddH<sub>2</sub>O, 10  $\mu$ mol in 0.5  $\mu$ L of forward or reverse primer, and 2  $\mu$ L of cDNA using the following procedure: 95 °C for 30 s, 95 °C for 5 s and 60 °C for 30 s for 45 cycles. Target gene expression was quantified relative to housekeeping gene (*GAPDH*) expression. Each RT-qPCR primer involved in the process is listed in Table S1 (Supplementary Materials).

### 2.9. Mitochondrial Membrane Potential ( $\Delta\Psi_m$ ) Assay

A  $\Delta\Psi_m$  assay was carried out using the  $\Delta\Psi_m$ -sensitive fluorescent probe 5,5',6,6'-tetrachloro-1,1',3,3'-tetraethyl-imidacarbocyanine iodide (JC-1; C2003S, Beyotime, Shanghai, China). Briefly, embryos were incubated with 2  $\mu$ M JC-1 for 30 min. After washing with PBS-PVA three times, the fluorescence signals were captured using a fluorescence microscope connected to a digital camera. The  $\Delta\Psi_m$  was calculated as the ratio of J-aggregate red fluorescence (red) to J-monomer green fluorescence (green). The fluorescence intensities of each embryo were analysed using NIH ImageJ software.

### 2.10. Intracellular Adenosine 5'-Triphosphate (ATP) Level Analysis

Briefly, embryos in each group ( $n = 40$ /per replicate) were lysed with 200  $\mu$ L of ATP-releasing reagent from an assay kit (S0027, Beyotime, Shanghai, China), sonicated on ice for 10 min and centrifuged at  $12,000\times g$  at 4 °C for 5 min. Next, ATP assay working solution was prepared by diluting ATP assay reagent with ATP assay diluent at a ratio of 1:4, and then 30  $\mu$ L of the supernatant was pipetted into a 96-well plate with a pipette together with 100  $\mu$ L of ATP working solution. Subsequently, chemiluminescence was detected using a microplate reader (Infinite M200 Pro, Tecan, Shanghai, China).

### 2.11. Statistical Analysis

For each experiment, at least three independent biological replicates were required. The data were evaluated using GraphPad 8.0.1 software (GraphPad, San Diego, CA, USA), and statistical comparisons of experiments were made using independent-sample *t* tests.

The data are presented as the mean  $\pm$  standard deviation (SD), and  $p < 0.05$  was considered to indicate statistical significance.

### 3. Results

#### 3.1. Effect of MA Supplementation at Various Concentrations on Porcine PA Embryo Development

To screen the optimum concentration of MA, parthenogenetically activated embryos were supplemented with different concentrations of MA (control, 1, 2 and 5  $\mu$ M), and the developmental performance of these embryos was analysed *in vitro*. The results indicated that none of the supplementation experimental groups showed any differences in cleavage rate (Figure 1B;  $p > 0.05$ ). At a concentration of 1  $\mu$ M, MA prominently increased the blastocyst formation rate on day 6 (Figure 1A,C;  $44.97 \pm 4.63\%$  vs.  $36.70 \pm 2.65\%$ ;  $p < 0.01$ ) and increased the rate of blastocyst hatching on day 7 (Figure 1D;  $12.31 \pm 2.38\%$  vs.  $8.03 \pm 2.09\%$ ;  $p < 0.05$ ) for the PA embryos compared with the embryos cultured in the non-supplemented group. Further analyses showed that 1  $\mu$ M MA not only increased the total cell numbers (Figure 1E,F;  $p < 0.05$ ) and cell proliferation (Figure 2A,B;  $p < 0.05$ ), but also decreased apoptosis occurrence (Figure 2C,D;  $p < 0.01$ ) in these embryos. Given these findings, 1  $\mu$ M MA was used in all subsequent experiments.

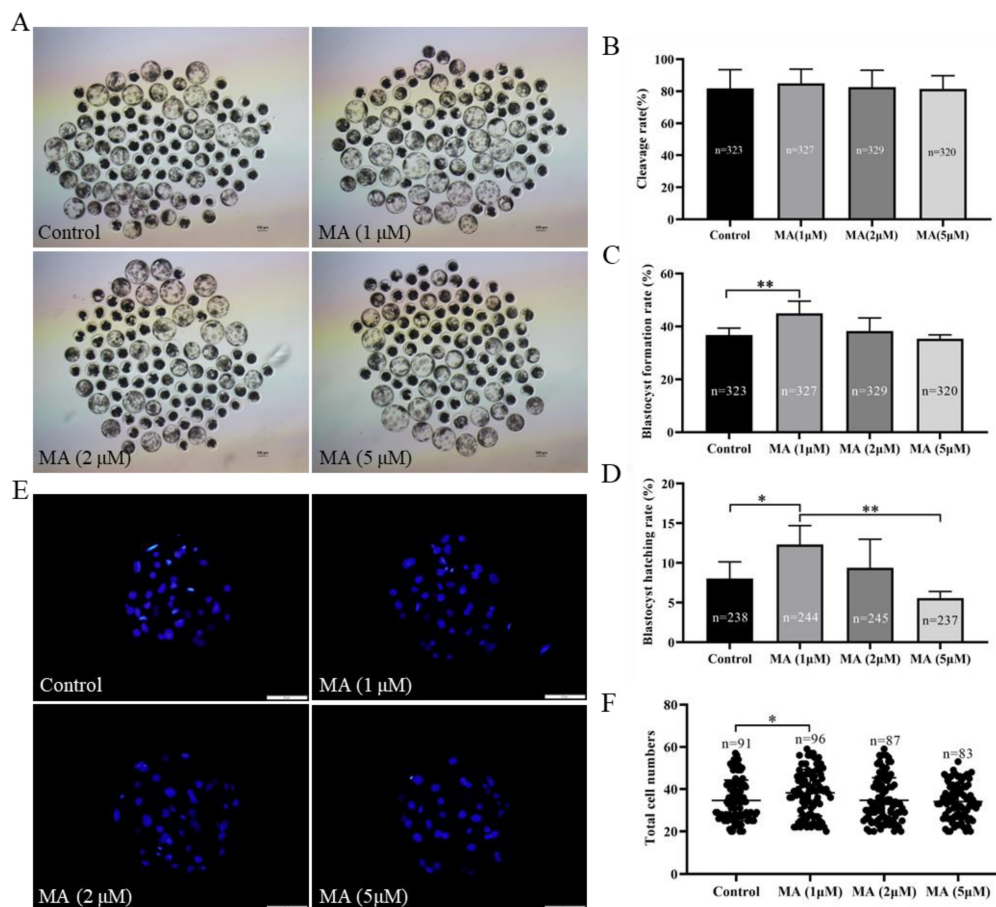


**Figure 1.** Effect of MA supplementation at various concentrations on the developmental performance of PA embryos. (A) Representative images of porcine PA embryonic development on day 6 in the control and MA supplementation groups. Scale bar = 100  $\mu$ m. (B) Cleavage rate of porcine parthenogenetic embryos on day 2. (C) Blastocyst formation rate of porcine PA embryos on day 6. (D) Blastocyst hatching rate of porcine PA embryos on day 7. (E) Representative fluorescence images of blastocyst staining with Hoechst 33342 on day 6 in the control and MA supplementation groups. Scale bar = 50  $\mu$ m. (F) Total cell numbers in blastocysts on day 6. The significant differences are represented with \* ( $p < 0.05$ ) and \*\* ( $p < 0.01$ ).



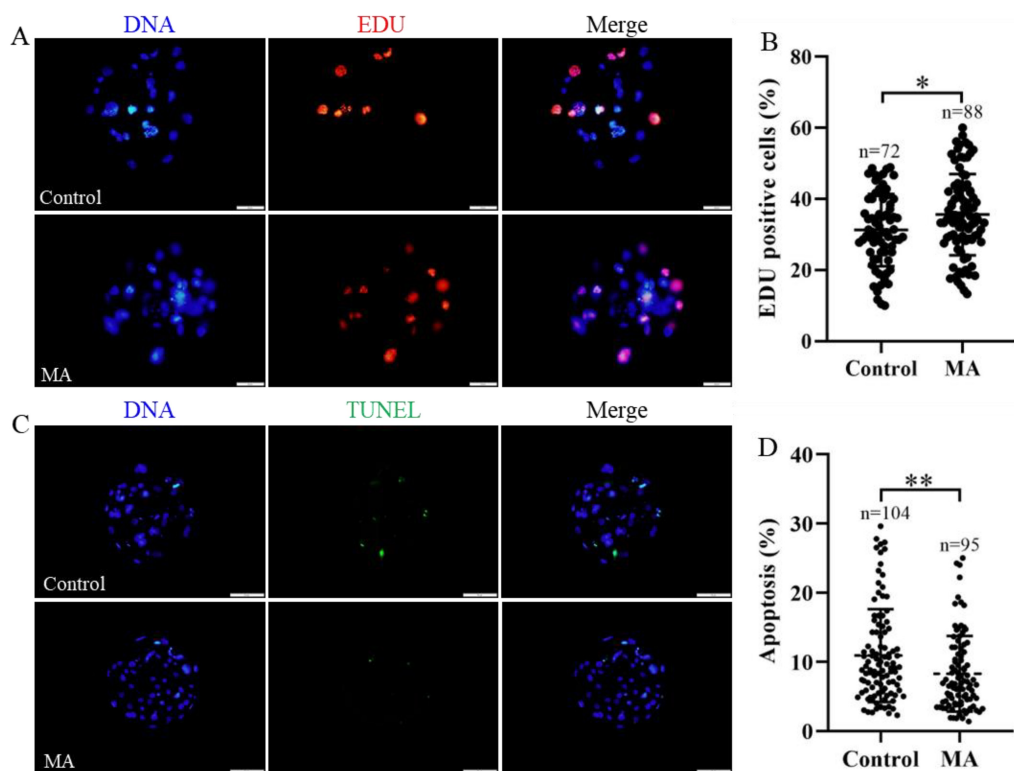


**Figure 2.** Effect of MA supplementation on cell proliferation and apoptosis in blastocysts derived from porcine parthenogenetic embryos. (A) Representative images of EDU-positive cells were detected in blastocysts. Scale bar = 20  $\mu\text{m}$ . (B) EDU-positive cell rate in blastocysts on day 6. (C) Representative images of TUNEL-positive cells detected in blastocysts. Scale bar = 50  $\mu\text{m}$ . (D) Apoptosis rate in blastocysts on day 6. The significant differences are represented with \* ( $p < 0.05$ ) and \*\* ( $p < 0.01$ ).

### 3.2. Effect of MA Supplementation on the In Vitro Developmental Potential of SCNT Embryos

Further analyses of the developmental potential of SCNT embryos *in vitro* demonstrated that MA supplementation in IVC prominently improved porcine SCNT embryo developmental competence. Compared with the control, the addition of 1  $\mu\text{M}$  MA to the culture medium did not affect the cleavage rate of SCNT embryos. (Figure 3B;  $p > 0.05$ ). Blastocyst formation rate was clearly higher in the MA-supplemented group than in the control group (Figure 3A,C;  $23.15 \pm 8.95\%$  vs.  $15.12 \pm 7.60\%$ ;  $p < 0.05$ ). Compared with the non-supplemented group, MA supplementation obviously increased the total cell numbers of blastocysts derived from SCNT embryos (Figure 3D,E;  $p < 0.05$ ).

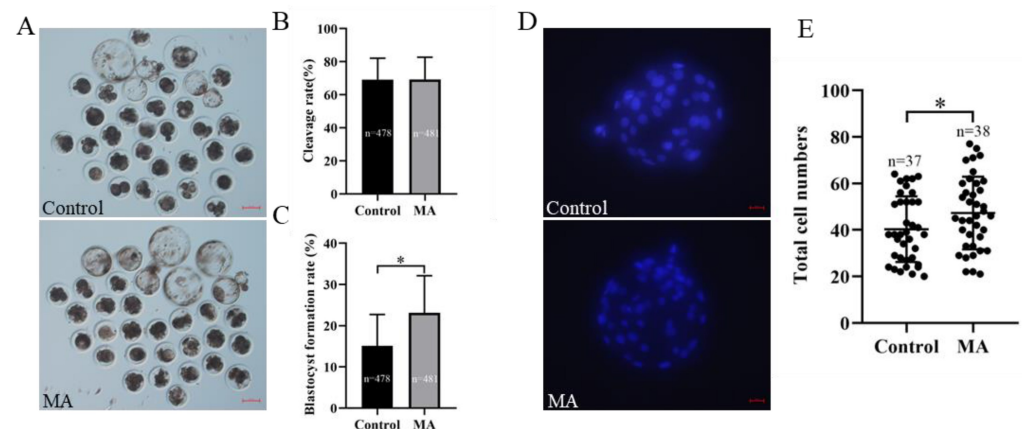


**Figure 3.** Effect of MA supplementation on the developmental competence of porcine SCNT embryos. (A) Representative images of porcine SCNT embryonic development on day 6 in the control and MA supplementation groups. Scale bar = 100  $\mu$ m. (B) Cleavage rate of porcine SCNT embryos on day 2. (C) Blastocyst formation rate of porcine SCNT embryos on day 6. (D) Representative fluorescence images of blastocyst staining with Hoechst 33342 on day 6 in the control and MA supplementation groups. Scale bar = 20  $\mu$ m. (E) Total cell numbers in blastocysts on day 6. The significant differences are represented with \* ( $p < 0.05$ ).

### 3.3. Effects of MA Supplementation on the Oxidation Resistance of Porcine Early-Stage Embryos

Because MA possesses free radical-scavenging properties, we hypothesized that MA supplementation would increase the resistance of porcine early-stage embryos to OS during the IVC period. The data showed that intracellular ROS abundance in porcine PA embryos was significantly lower at the 4-cell stage (Figure 4A,C;  $p < 0.01$ ) and blastocyst stage (Figure 4B,D;  $p < 0.0001$ ) in the MA supplementation group than in the non-supplemented group. In addition, under oxidative damage conditions, MA supplementation significantly attenuated intracellular ROS levels in porcine parthenogenetic embryos at the 4-cell stage during IVC (Figure S1A,C;  $p < 0.0001$ ) and blastocyst stage (Figure S1B,D;  $p < 0.01$ ) compared with those in the  $H_2O_2$ -exposed group. Further analysis showed that MA supplementation during IVC increased intracellular GSH abundance in 4-cell embryos (Figure 4E,G;  $p < 0.0001$ ) and blastocyst stage (Figure 4F,H;  $p < 0.01$ ). Western blotting showed that the pluripotency factor octamer-binding transcription factor 4 (OCT4) and antioxidant factors superoxide dismutase 1 (SOD1) and catalase (CAT) were upregulated in the MA supplementation group compared with the non-supplemented group of porcine PA embryos at day 6 (Figure 5). Subsequent RT-qPCR analyses showed that the relative mRNA expression levels of anti-apoptotic gene B-cell lymphoma 2 (*BCL2*), antioxidant-related gene haem oxygenase-1 (*HO-1*) and cell proliferation-related gene dihydroorotate dehydrogenase (*DHODH*) were significantly upregulated, while that of pro-apoptotic gene BCL2-associated X protein (*BAX*) was significantly downregulated, in the MA supplementation group compared with the non-supplemented group of porcine PA embryos at day 6 (Figure S2). These results indicated that MA supplementation could increase the OS resistance of porcine early-stage embryos during the IVC period.

### 3.4. Effects of MA Supplementation during IVC on the Mitochondrial Function of Porcine Early-Stage Embryos

Excess generation of ROS is associated with mitochondrial dysfunction. Thus, the  $\Delta\Psi_m$  and intracellular ATP levels in porcine parthenogenetic embryos were analysed. The  $\Delta\Psi_m$  was assayed using the JC-1 fluorescence reaction. Quantitative analysis demonstrated that MA significantly increased the relative ratio of JC-1 fluorescence intensity (red/green) in the MA supplementation group compared with the non-supplemented group of porcine blastocysts derived from PA embryos (Figure 6A,B;  $p < 0.01$ ). Furthermore, analysis indicated that MA supplementation during IVC also led to dramatic increases in intracellular

ATP levels (Figure 6C;  $p < 0.0001$ ). These results suggested that MA supplementation could effectively improve the mitochondrial function of porcine early-stage embryos.

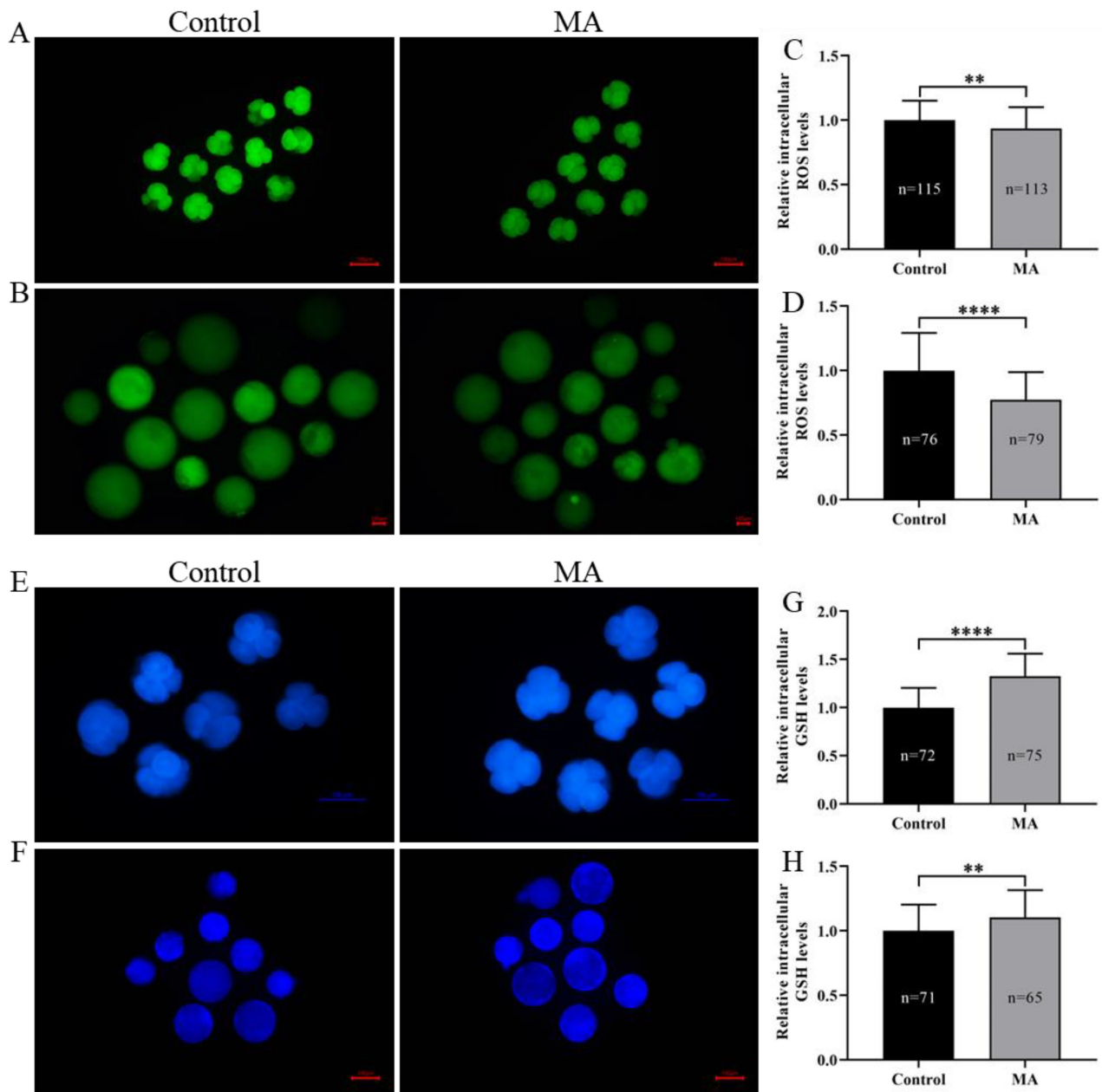


**Figure 4.** Effect of MA supplementation on antioxidation ability in porcine parthenogenetic embryos. Representative fluorescence images of intracellular ROS in PA embryos at the 4-cell (A) and blastocyst (B) stages in the control and MA supplementation groups. Scale bar = 100  $\mu$ m. Relative intracellular ROS levels in 4-cell (C) and blastocyst (D) stage embryos. Representative fluorescence images of intracellular GSH in parthenogenetic embryos at the 4-cell (E) and blastocyst (F) stages in the control and MA supplementation groups. Scale bar = 100  $\mu$ m. Relative intracellular GSH levels in 4-cell (G) and blastocyst (H) stage embryos. The significant differences are represented with \*\* ( $p < 0.01$ ) and \*\*\*\* ( $p < 0.0001$ ).



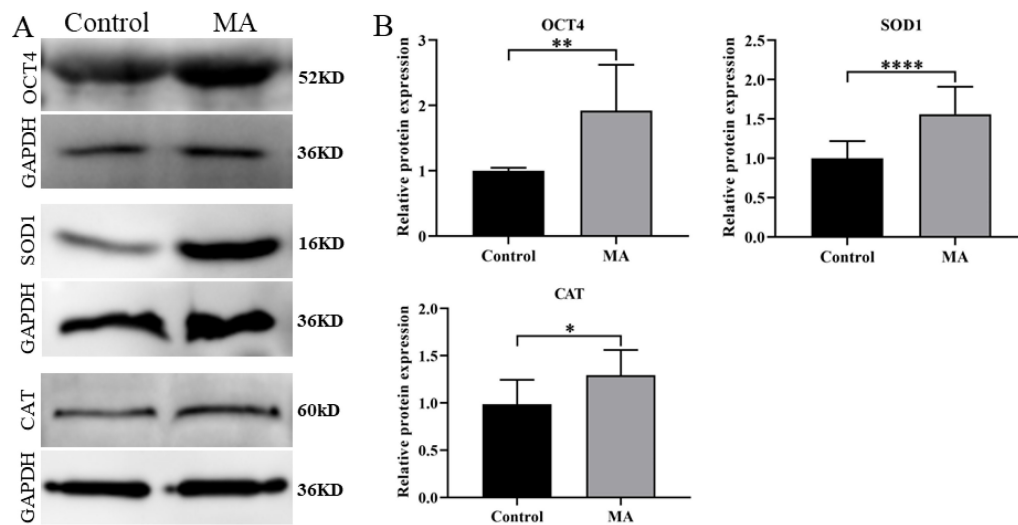


**Figure 5.** (A) Western blotting analysis of OCT4, SOD1 and CAT expression in porcine parthenogenetic embryos in the control and MA supplementation groups. (B) Relative expression of OCT4, SOD1 and CAT levels in porcine parthenogenetic embryos. The significant differences are represented with \* ( $p < 0.05$ ), \*\* ( $p < 0.01$ ), \*\*\*\* ( $p < 0.0001$ ).

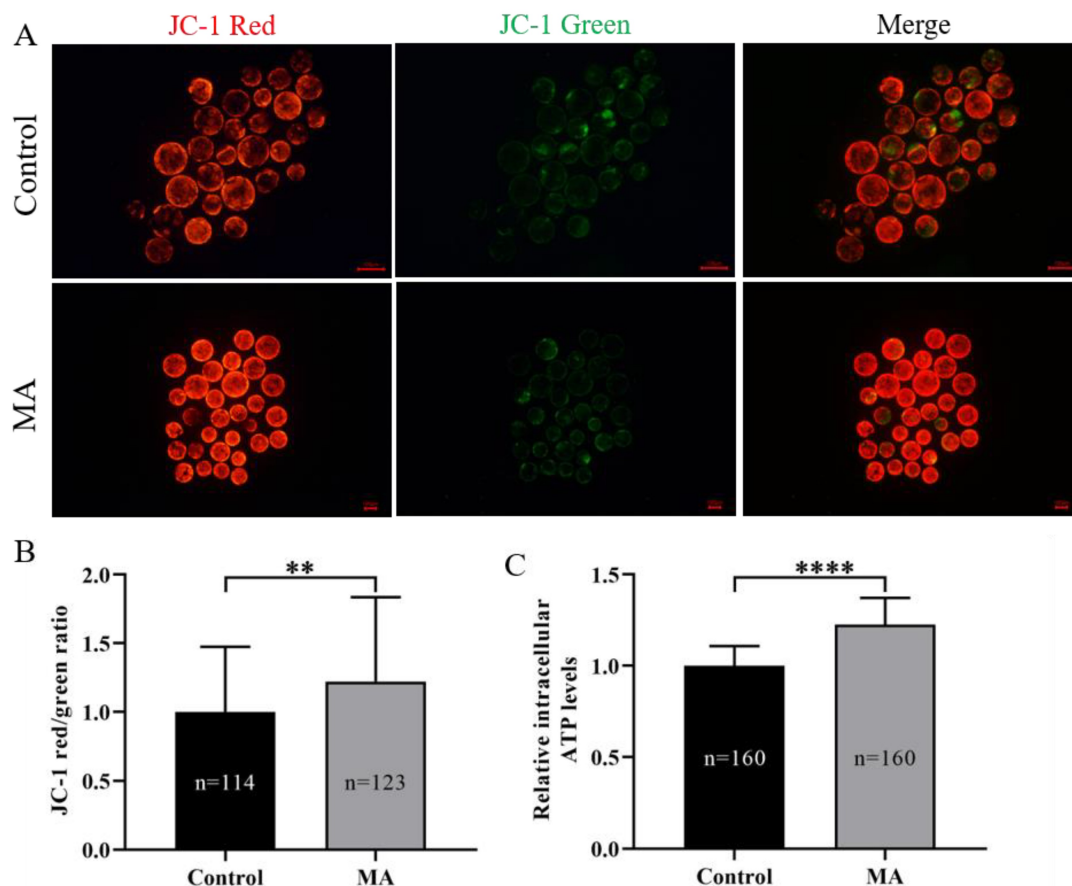


**Figure 6.** Effect of MA supplementation on  $\Delta\Psi$ m and intracellular ATP levels in porcine parthenogenetic embryos. (A) Representative fluorescent images of JC-1 staining in porcine PA embryos at the blastocyst stage in the control and MA supplementation groups. Scale bar = 100  $\mu$ m. (B) Relative fluorescence intensity of JC-1 in the blastocyst-stage embryos. (C) Relative intracellular ATP levels in blastocyst-stage embryos. The significant differences are represented with \*\* ( $p < 0.01$ ) and \*\*\*\* ( $p < 0.0001$ ).

#### 4. Discussion

During IVC of early-stage embryos, OS often impairs embryo development rate and quality [39]. This paper has indicated evidence to show that MA, a natural antioxidant, promotes the developmental performance of PA and SCNT embryos to blastocysts during the IVC period. This beneficial effect occurred because MA effectively alleviated OS, promoted cell proliferation, reduced apoptosis levels and stabilized mitochondrial function, suggesting that MA can ameliorate the developmental competence of early-stage embryos by enhancing oxidation resistance.

Previous studies have already confirmed that MA has antioxidative effects in several other cell types, including human umbilical vein endothelial cells [27], vascular smooth muscle cells [35], human healthy peripheral blood mononuclear cells [40] and pheochromocytoma cells [31]; however, the present study is the first to evaluate the effect of MA on the *in vitro* development of porcine PA and SCNT embryos during the early stage in IVC with prolonged ROS accumulation. Our data showed that supplementation with 1  $\mu$ M MA markedly increased the development rate and quality of porcine early-stage embryos, as demonstrated by improved blastocyst formation, hatching and total cell numbers; promoted proliferation; reduced apoptosis; and increased  $\Delta\Psi_m$  and ATP levels. Importantly, the abundance of intracellular ROS was dramatically decreased and the abundance of intracellular GSH was greatly increased in the MA group. These beneficial effects of MA on the development of early-stage embryos may involve the antioxidant and antiapoptotic properties of MA.

To further explore why MA promotes porcine early-stage embryo development, we used EDU labelling of blastocyst cells, and the results revealed that MA supplementation obviously increased the cell proliferation rate of blastocysts. MA is known to effectively exert pro-proliferative and antiapoptotic influences on somatic cells at a relatively low dose [34]. Similarly, the apoptotic cell numbers of the MA group blastocysts were clearly fewer than the numbers of the non-supplemented group in the present study. *BCL2*-family genes, especially *BAX* and *BCL2*, are key regulators of apoptosis, and their main sites of action are mitochondria [41]. The downregulation of the proapoptotic gene *BAX* and upregulation of the antiapoptotic gene *BCL2* in the MA group also supported our hypothesis [42]. In addition, OCT4 plays a vital role in both cell fate decisions and cell proliferation in porcine early-stage embryos [43], while knockout of OCT4 inhibits blastocyst development [44]. Therefore, the OCT4 expression level is positively related to blastocyst pluripotency. The study also showed that OCT4 was notably upregulated in the MA addition group compared with the non-supplemented group.

Overaccumulation of ROS has adverse effects on cells through damage to cellular lipids [45], DNA and organelles [46], as well as alterations in enzymatic function [47], proliferation and apoptosis [48]. Accordingly, maintaining a dynamic balance between antioxidant and ROS levels is pivotal for high embryo development. GSH, a tripeptide of  $\gamma$ -glutamylcysteinylglycine, is an endogenous antioxidant that contributes to both enzyme-dependent and non-enzymatic dependent against OS [49], and is an ineffective substrate for SOD1-catalysed  $H_2O_2$  formation in cells and tissues [50]. A lack of GSH can cause an increase in intracellular ROS generation [51], embryonic apoptosis sensitivity [52] and expended mitochondrial damage [53], and high intracellular GSH levels can improve the developmental competence of embryos by reducing intracellular ROS levels and changing the apoptosis coefficient [54]. In this paper, MA supplementation clearly decreased ROS levels, even under oxidative damage conditions, and evidently increased GSH levels in porcine early-stage embryos, which is consistent with the results of other studies [32]. SOD1 and CAT are crucial enzymatic antioxidants for ROS scavenging [55]; SOD can resolve into a superoxide to oxygen and hydrogen peroxide, which is then converted to water and oxygen by CAT. A prior study reported that MA increases the activity of these enzymes in healthy A10 cells following treatment with  $H_2O_2$  [56]. In the present study, SOD1 and CAT levels were markedly higher in the MA group than in the non-supplemented group when porcine zygotes developed to the blastocyst stage. SOD1 and CAT expression

were upregulated. Additionally, it has previously been reported that MA protects VSMCs against OS through the *Akt/Nrf2/HO-1* pathway activation [35], and *HO-1* is one of the most critical genes regulated by *Nrf2* [57]. Moreover, it is generally acknowledged that *HO-1* deficiency is attributed to embryonic death, and previous studies have confirmed the role of *HO-1* in embryonic survival [58]. Consequently, the mRNA expression level of *HO-1* was significantly upregulated, and these results indicated that the antioxidant capacity of blastocysts was greatly improved in the MA group. Hence, MA played a positive role in protecting porcine early-stage embryos from OS by enhancing oxidation resistance.

In addition to scavenging of ROS directly, MA could also maintain mitochondrial stability [59]. Mitochondria are essential organelles during early embryonic development, and mitochondrial dysfunction is associated with failure of embryonic development [60].  $\Delta\Psi_m$  is commonly used as an indicator of mitochondrial function and cellular viability in embryos [61]. A normal  $\Delta\Psi_m$  is necessary for mitochondrial ATP production [62] and oxidative phosphorylation [63]. When  $\Delta\Psi_m$  decreases, mitochondrial permeability increases [64], ATP synthesis decreases [65], cytochrome c is released [66], intracellular oxidative reduction is altered and *BCL2* gene family members intervene to accelerate apoptosis [67]. Importantly, the release of mitochondrial membrane proteins and the dissipation of  $\Delta\Psi_m$  occur frequently in disease states with increased cell death [68]. In our study, MA-treated embryos exhibited dramatically increased  $\Delta\Psi_m$  and ATP levels. In both prokaryotes and eukaryotes, DHODH is the only enzyme in pyrimidine biosynthesis located in the mitochondria rather than the cell membranes [69]; it acts on cell proliferation and has a physical connection with respiratory complexes. Loss of DHODH leads to mitochondrial dysfunction. DHODH deficiency partially inhibited mitochondrial respiratory chain complex III, decreased  $\Delta\Psi_m$ , and increased ROS production [70]. The upregulation of *DHODH* expression further proved that MA could improve mitochondrial function and cell proliferation in blastocysts.

## 5. Conclusions

The present context suggests that MA can enhance the developmental capacity *in vitro* of porcine early-stage embryos by eliminating OS, enhancing mitochondrial function, promoting proliferation and inhibiting apoptosis, thereby improving the developmental efficiency of early embryos during the IVC period. Therefore, MA is a potential candidate natural antioxidant that can be used to improve the potential of porcine early-stage embryo IVC. In the future, these findings may be verified in *in vitro*-produced porcine embryos and, ultimately, in *in vivo* studies.

**Supplementary Materials:** The following supporting information can be downloaded at: <https://www.mdpi.com/article/10.3390/ani13061041/s1>, Figure S1: MA supplementation reduces H<sub>2</sub>O<sub>2</sub>-induced intracellular ROS levels in porcine parthenogenetic embryos; Figure S2: Relative mRNA expression of *BCL2*, *BAX*, *HO-1* and *DHODH* in porcine parthenogenetic embryos in the control and MA supplementation groups. Table S1: Sequences of primers used for RT-qPCR.

**Author Contributions:** Conceptualization, T.-T.Y., J.-J.Q., B.-X.S. and S.L.; Methodology, T.-T.Y., J.-J.Q., B.-X.S. and S.L.; Investigation, T.-T.Y., J.-J.Q., H.-X.Q. and H.-K.W.; Visualization, T.-T.Y., J.-J.Q., H.-X.Q. and H.-K.W.; Data curation and formal analysis, T.-T.Y., S.L., H.S., H.J. and J.-B.Z.; Writing, T.-T.Y., J.-J.Q. and S.L. All authors have read and agreed to the published version of the manuscript.

**Funding:** This research was supported by the Jilin Scientific and Technological Development Program of China (20210202027NC, 2021–2024).

**Institutional Review Board Statement:** This study was approved by the Institutional Animal Care and Use Committee of Jilin University, Changchun, China (SY202302030).

**Informed Consent Statement:** Not applicable.

**Data Availability Statement:** The dataset generated and/or analysed during the current study is available from the corresponding author on reasonable request.

**Conflicts of Interest:** The authors declare no conflict of interest.

## References

1. Zhao, J.; Ross, J.W.; Hao, Y.; Spate, L.D.; Walters, E.M.; Samuel, M.S.; Rieke, A.; Murphy, C.N.; Prather, R.S. Significant improvement in cloning efficiency of an inbred miniature pig by histone deacetylase inhibitor treatment after somatic cell nuclear transfer. *Biol. Reprod.* **2009**, *81*, 525–530. [\[CrossRef\]](#) [\[PubMed\]](#)
2. Ren, J.; Yu, D.; Wang, J.; Xu, K.; Xu, Y.; Sun, R.; An, P.; Li, C.; Feng, G.; Zhang, Y.; et al. Generation of immunodeficient pig with hereditary tyrosinemia type 1 and their preliminary application for humanized liver. *Cell Biosci.* **2022**, *12*, 26. [\[CrossRef\]](#) [\[PubMed\]](#)
3. van der Weijden, V.A.; Schmidhauser, M.; Kurome, M.; Knubben, J.; Flöter, V.L.; Wolf, E.; Ulbrich, S.E. Transcriptome dynamics in early in vivo developing and in vitro produced porcine embryos. *BMC Genom.* **2021**, *22*, 139. [\[CrossRef\]](#) [\[PubMed\]](#)
4. Kikuchi, K.; Onishi, A.; Kashiwazaki, N.; Iwamoto, M.; Noguchi, J.; Kaneko, H.; Akita, T.; Nagai, T. Successful piglet production after transfer of blastocysts produced by a modified in vitro system. *Biol. Reprod.* **2002**, *66*, 1033–1041. [\[CrossRef\]](#) [\[PubMed\]](#)
5. Rath, D.; Niemann, H.; Torres, C.R. In vitro development to blastocysts of early porcine embryos produced in vivo or in vitro. *Theriogenology* **1995**, *43*, 913–926. [\[CrossRef\]](#)
6. Martinez, C.A.; Cuello, C.; Parrilla, I.; Maside, C.; Ramis, G.; Cambra, J.M.; Vazquez, J.M.; Rodriguez-Martinez, H.; Gil, M.A.; Martinez, E.A. Exogenous Melatonin in the Culture Medium Does Not Affect the Development of In Vivo-Derived Pig Embryos but Substantially Improves the Quality of In Vitro-Produced Embryos. *Antioxidants* **2022**, *11*, 1177. [\[CrossRef\]](#)
7. Leite, R.F.; Annes, K.; Ispada, J.; de Lima, C.B.; Dos Santos, É.C.; Fontes, P.K.; Nogueira, M.F.G.; Milazzotto, M.P. Oxidative Stress Alters the Profile of Transcription Factors Related to Early Development on In Vitro Produced Embryos. *Oxid. Med. Cell Longev.* **2017**, *2017*, 1502489. [\[CrossRef\]](#)
8. Lebuffe, G.; Schumacker, P.T.; Shao, Z.H.; Anderson, T.; Iwase, H.; Vanden Hoek, T.L. ROS and NO trigger early preconditioning: Relationship to mitochondrial KATP channel. *Am. J. Physiol. Heart Circ. Physiol.* **2003**, *284*, H299–H308. [\[CrossRef\]](#)
9. Li, Y.; Chen, H.; Liao, J.; Chen, K.; Javed, M.T.; Qiao, N.; Zeng, Q.; Liu, B.; Yi, J.; Tang, Z.; et al. Long-term copper exposure promotes apoptosis and autophagy by inducing oxidative stress in pig testis. *Environ. Sci. Pollut. Res. Int.* **2021**, *28*, 55140–55153. [\[CrossRef\]](#)
10. Romek, M.; Gajda, B.; Krzysztofowicz, E.; Smorag, Z. Changes of lipid composition in non-cultured and cultured porcine embryos. *Theriogenology* **2010**, *74*, 265–276. [\[CrossRef\]](#)
11. Lee, K.; Wang, C.; Chaille, J.M.; Machaty, Z. Effect of resveratrol on the development of porcine embryos produced in vitro. *J. Reprod. Dev.* **2010**, *56*, 330–335. [\[CrossRef\]](#) [\[PubMed\]](#)
12. Niu, Y.J.; Zhou, W.; Nie, Z.W.; Shin, K.T.; Cui, X.S. Melatonin enhances mitochondrial biogenesis and protects against rotenone-induced mitochondrial deficiency in early porcine embryos. *J. Pineal Res.* **2020**, *68*, e12627. [\[CrossRef\]](#) [\[PubMed\]](#)
13. Liang, S.; Jin, Y.X.; Yuan, B.; Zhang, J.B.; Kim, N.H. Melatonin enhances the developmental competence of porcine somatic cell nuclear transfer embryos by preventing DNA damage induced by oxidative stress. *Sci. Rep.* **2017**, *7*, 11114. [\[CrossRef\]](#)
14. Hu, J.; Cheng, D.; Gao, X.; Bao, J.; Ma, X.; Wang, H. Vitamin C enhances the in vitro development of porcine pre-implantation embryos by reducing oxidative stress. *Reprod. Domest. Anim.* **2012**, *47*, 873–879. [\[CrossRef\]](#) [\[PubMed\]](#)
15. Jiang, H.; Liang, S.; Yao, X.R.; Jin, Y.X.; Shen, X.H.; Yuan, B.; Zhang, J.B.; Kim, N.H. Laminarin improves developmental competence of porcine early stage embryos by inhibiting oxidative stress. *Theriogenology* **2018**, *115*, 38–44. [\[CrossRef\]](#)
16. Qi, J.J.; Li, X.X.; Diao, Y.F.; Liu, P.L.; Wang, D.L.; Bai, C.Y.; Yuan, B.; Liang, S.; Sun, B.X. Asiatic acid supplementation during the in vitro culture period improves early embryonic development of porcine embryos produced by parthenogenetic activation, somatic cell nuclear transfer and in vitro fertilization. *Theriogenology* **2020**, *142*, 26–33. [\[CrossRef\]](#)
17. Xie, P.; Huang, L.; Zhang, C.; Deng, Y.; Wang, X.; Cheng, J. Enhanced extraction of hydroxytyrosol, maslinic acid and oleanolic acid from olive pomace: Process parameters, kinetics and thermodynamics, and greenness assessment. *Food Chem.* **2019**, *276*, 662–674. [\[CrossRef\]](#)
18. Alvarez, M.E.; Rotelli, A.E.; Pelzer, L.E.; Saad, J.R.; Giordano, O. Phytochemical study and anti-inflammatory properties of *Lampaya hieronymi* Schum. ex Moldenke. *Il Farmaco* **2000**, *55*, 502–505.
19. Yi, J.-H.; Zhang, G.-L.; Li, B.-G.; Chen, Y.-Z. Two glycosides from the stem bark of *Tetracentron sinense*. *Phytochemistry* **2000**, *53*, 1001–1003. [\[CrossRef\]](#)
20. Xu, H.-X.; Zeng, F.-Q.; Wan, M.; Sim, K.-Y. Anti-HIV Triterpene Acids from *Geum japonicum*. *J. Nat. Prod.* **1996**, *59*, 643–645. [\[CrossRef\]](#)
21. Serbian, I.; Siewert, B.; Al-Harrasi, A.; Csuk, R. 2-O-(2-chlorobenzoyl) maslinic acid triggers apoptosis in A2780 human ovarian carcinoma cells. *Eur. J. Med. Chem.* **2019**, *180*, 457–464. [\[CrossRef\]](#) [\[PubMed\]](#)
22. Hsia, T.C.; Liu, W.H.; Qiu, W.W.; Luo, J.; Yin, M.C. Maslinic acid induces mitochondrial apoptosis and suppresses HIF-1 $\alpha$  expression in A549 lung cancer cells under normoxic and hypoxic conditions. *Molecules* **2014**, *19*, 19892–19906. [\[CrossRef\]](#) [\[PubMed\]](#)
23. Hung, Y.-C.; Yang, H.-T.; Yin, M.-C. Asiatic acid and maslinic acid protected heart via anti-glycative and anti-coagulatory activities in diabetic mice. *Food Funct.* **2015**, *6*, 2967–2974. [\[CrossRef\]](#) [\[PubMed\]](#)
24. Soltane, R.; Chrouda, A.; Mostafa, A.; Al-Karmalawy, A.A.; Chouaib, K.; Dhahri, A.; Pashameah, R.A.; Alasiri, A.; Kutkat, O.; Shehata, M.; et al. Strong Inhibitory Activity and Action Modes of Synthetic Maslinic Acid Derivative on Highly Pathogenic Coronaviruses: COVID-19 Drug Candidate. *Pathogens* **2021**, *10*, 623. [\[CrossRef\]](#) [\[PubMed\]](#)



25. Blanco-Cabra, N.; Vega-Granados, K.; Moya-Anderico, L.; Vukomanovic, M.; Parra, A.; Alvarez de Cienfuegos, L.; Torrents, E. Novel Oleanolic and Maslinic Acid Derivatives as a Promising Treatment against Bacterial Biofilm in Nosocomial Infections: An in Vitro and in Vivo Study. *ACS Infect. Dis.* **2019**, *5*, 1581–1589. [\[CrossRef\]](#)
26. Huang, L.; Guan, T.; Qian, Y.; Huang, M.; Tang, X.; Li, Y.; Sun, H. Anti-inflammatory effects of maslinic acid, a natural triterpene, in cultured cortical astrocytes via suppression of nuclear factor-kappa B. *Eur. J. Pharmacol.* **2011**, *672*, 169–174. [\[CrossRef\]](#)
27. Lee, W.; Kim, J.; Park, E.K.; Bae, J.S. Maslinic Acid Ameliorates Inflammation via the Downregulation of NF-kappaB and STAT-1. *Antioxidants* **2020**, *9*, 106. [\[CrossRef\]](#)
28. Chen, Y.L.; Yan, D.Y.; Wu, C.Y.; Xuan, J.W.; Jin, C.Q.; Hu, X.L.; Bao, G.D.; Bian, Y.J.; Hu, Z.C.; Shen, Z.H.; et al. Maslinic acid prevents IL-1beta-induced inflammatory response in osteoarthritis via PI3K/AKT/NF-kappaB pathways. *J. Cell Physiol.* **2021**, *236*, 1939–1949. [\[CrossRef\]](#)
29. Kim, K.M.; Kim, J.; Baek, M.C.; Bae, J.S. Novel factor Xa inhibitor, maslinic acid, with antiplatelet aggregation activity. *J. Cell Physiol.* **2020**, *235*, 9445–9456. [\[CrossRef\]](#)
30. Aladedunye, F.A.; Okorie, D.A.; Ighodaro, O.M. Anti-inflammatory and antioxidant activities and constituents of *Platostoma africanum* P. Beauv. *Nat. Prod. Res.* **2008**, *22*, 1067–1073. [\[CrossRef\]](#)
31. Marquez Martin, A.; de la Puerta Vazquez, R.; Fernandez-Arche, A.; Ruiz-Gutierrez, V. Suppressive effect of maslinic acid from pomace olive oil on oxidative stress and cytokine production in stimulated murine macrophages. *Free Radic. Res.* **2006**, *40*, 295–302. [\[CrossRef\]](#) [\[PubMed\]](#)
32. Alsabaani, N.A.; Osman, O.M.; Dallak, M.A.; Morsy, M.D.; Al-Dhibi, H.A. Maslinic Acid Protects against Streptozotocin-Induced Diabetic Retinopathy by Activating Nrf2 and Suppressing NF-kappaB. *J. Ophthalmol.* **2022**, *2022*, 3044202. [\[CrossRef\]](#) [\[PubMed\]](#)
33. Velasco, J.; Holgado, F.; Márquez-Ruiz, G.; Ruiz-Méndez, M.V. Concentrates of triterpenic acids obtained from crude olive pomace oils: Characterization and evaluation of their potential antioxidant activity. *J. Sci. Food Agric.* **2018**, *98*, 4837–4844. [\[CrossRef\]](#) [\[PubMed\]](#)
34. Li, F.; Li, Q.; Shi, X.; Guo, Y. Maslinic acid inhibits impairment of endothelial functions induced by high glucose in HAEC cells through improving insulin signaling and oxidative stress. *Biomed. Pharmacother.* **2017**, *95*, 904–913. [\[CrossRef\]](#)
35. Qin, X.; Qiu, C.; Zhao, L. Maslinic acid protects vascular smooth muscle cells from oxidative stress through Akt/Nrf2/HO-1 pathway. *Mol. Cell. Biochem.* **2014**, *390*, 61–67. [\[CrossRef\]](#)
36. Mkhwanazi, B.N.; Serumula, M.R.; Myburg, R.B.; Van Heerden, F.R.; Musabayane, C.T. Antioxidant effects of maslinic acid in livers, hearts and kidneys of streptozotocin-induced diabetic rats: Effects on kidney function. *Ren. Fail.* **2014**, *36*, 419–431. [\[CrossRef\]](#)
37. Hu, W.; Zhang, Y.; Wang, D.; Yang, T.; Qi, J.; Zhang, Y.; Jiang, H.; Zhang, J.; Sun, B.; Liang, S. Iron Overload-Induced Ferroptosis Impairs Porcine Oocyte Maturation and Subsequent Embryonic Developmental Competence in vitro. *Front. Cell Dev. Biol.* **2021**, *9*, 673291. [\[CrossRef\]](#)
38. Liang, S.; Zhao, M.H.; Choi, J.W.; Kim, N.H.; Cui, X.S. Scriptaid Treatment Decreases DNA Methyltransferase 1 Expression by Induction of MicroRNA-152 Expression in Porcine Somatic Cell Nuclear Transfer Embryos. *PLoS ONE* **2015**, *10*, e0134567. [\[CrossRef\]](#)
39. Shih, Y.F.; Lee, T.H.; Liu, C.H.; Tsao, H.M.; Huang, C.C.; Lee, M.S. Effects of reactive oxygen species levels in prepared culture media on embryo development: A comparison of two media. *Taiwan J. Obstet. Gynecol.* **2014**, *53*, 504–508. [\[CrossRef\]](#)
40. Banerjee, J.; Hasan, S.N.; Samanta, S.; Giri, B.; Bag, B.G.; Dash, S.K. Self-Assembled Maslinic Acid Attenuates Doxorubicin Induced Cytotoxicity via Nrf2 Signaling Pathway: An In Vitro and In Silico Study in Human Healthy Cells. *Cell Biochem. Biophys.* **2022**, *80*, 563–578. [\[CrossRef\]](#)
41. Liu, S.; Pereira, N.A.; Teo, J.J.; Miller, P.; Shah, P.; Song, Z. Mitochondrially targeted Bcl-2 and Bcl-X(L) chimeras elicit different apoptotic responses. *Mol. Cells* **2007**, *24*, 378–387. [\[PubMed\]](#)
42. Li, T.; Wang, H.; Dong, S.; Liang, M.; Ma, J.; Jiang, X.; Yu, W. Protective effects of maslinic acid on high fat diet-induced liver injury in mice. *Life Sci.* **2022**, *301*, 120634. [\[CrossRef\]](#) [\[PubMed\]](#)
43. Lee, M.; Oh, J.N.; Choe, G.C.; Kim, S.H.; Choi, K.H.; Lee, D.K.; Jeong, J.; Lee, C.K. Changes in OCT4 expression play a crucial role in the lineage specification and proliferation of preimplantation porcine blastocysts. *Cell Prolif.* **2022**, *55*, e13313. [\[CrossRef\]](#) [\[PubMed\]](#)
44. Tan, M.H.; Au, K.F.; Leong, D.E.; Foygel, K.; Wong, W.H.; Yao, M.W. An Oct4-Sall4-Nanog network controls developmental progression in the pre-implantation mouse embryo. *Mol. Syst. Biol.* **2013**, *9*, 632. [\[CrossRef\]](#)
45. Komninou, E.R.; Remião, M.H.; Lucas, C.G.; Domingues, W.B.; Basso, A.C.; Jornada, D.S.; Deschamps, J.C.; Beck, R.C.; Pohlmann, A.R.; Bordignon, V.; et al. Effects of Two Types of Melatonin-Loaded Nanocapsules with Distinct Supramolecular Structures: Polymeric (NC) and Lipid-Core Nanocapsules (LNC) on Bovine Embryo Culture Model. *PLoS ONE* **2016**, *11*, e0157561. [\[CrossRef\]](#)
46. Qian, D.; Li, Z.; Zhang, Y.; Huang, Y.; Wu, Q.; Ru, G.; Chen, M.; Wang, B. Response of Mouse Zygotes Treated with Mild Hydrogen Peroxide as a Model to Reveal Novel Mechanisms of Oxidative Stress-Induced Injury in Early Embryos. *Oxid. Med. Cell Longev.* **2016**, *2016*, 1521428. [\[CrossRef\]](#)
47. Brennan, L.A.; Steinhorn, R.H.; Wedgwood, S.; Mata-Greenwood, E.; Roark, E.A.; Russell, J.A.; Black, S.M. Increased superoxide generation is associated with pulmonary hypertension in fetal lambs: A role for NADPH oxidase. *Circ. Res.* **2003**, *92*, 683–691. [\[CrossRef\]](#)



48. Gao, X.; Li, X.; Wang, Z.; Li, K.; Liang, Y.; Yao, X.; Zhang, G.; Wang, F. l-Arginine regulates the proliferation, apoptosis and endocrine activity by alleviating oxidative stress in sheep endometrial epithelial cells. *Theriogenology* **2022**, *179*, 187–196. [\[CrossRef\]](#)
49. Schafer, F.Q.; Buettner, G.R. Redox environment of the cell as viewed through the redox state of the glutathione disulfide/glutathione couple. *Free Radic. Biol. Med.* **2001**, *30*, 1191–1212. [\[CrossRef\]](#)
50. Bakavayev, S.; Chetrit, N.; Zvagelsky, T.; Mansour, R.; Vyazmensky, M.; Barak, Z.; Israelson, A.; Engel, S. Cu/Zn-superoxide dismutase and wild-type like fALS SOD1 mutants produce cytotoxic quantities of H<sub>2</sub>O<sub>2</sub> via cysteine-dependent redox short-circuit. *Sci. Rep.* **2019**, *9*, 10826. [\[CrossRef\]](#)
51. Dickerhof, N.; Pearson, J.F.; Hoskin, T.S.; Berry, L.J.; Turner, R.; Sly, P.D.; Kettle, A.J.; Arest, C.F. Oxidative stress in early cystic fibrosis lung disease is exacerbated by airway glutathione deficiency. *Free Radic. Biol. Med.* **2017**, *113*, 236–243. [\[CrossRef\]](#) [\[PubMed\]](#)
52. Lim, J.; Luderer, U. Glutathione deficiency sensitizes cultured embryonic mouse ovaries to benzo[a]pyrene-induced germ cell apoptosis. *Toxicol. Appl. Pharmacol.* **2018**, *352*, 38–45. [\[CrossRef\]](#) [\[PubMed\]](#)
53. Shi, Z.Z.; Osei-Frimpong, J.; Kala, G.; Kala, S.V.; Barrios, R.J.; Habib, G.M.; Lukin, D.J.; Danney, C.M.; Matzuk, M.M.; Lieberman, M.W. Glutathione synthesis is essential for mouse development but not for cell growth in culture. *Proc. Natl. Acad. Sci. USA* **2000**, *97*, 5101–5106. [\[CrossRef\]](#) [\[PubMed\]](#)
54. Li, X.X.; Lee, K.B.; Lee, J.H.; Kim, K.J.; Kim, E.Y.; Han, K.W.; Park, K.S.; Yu, J.; Kim, M.K. Glutathione and cysteine enhance porcine preimplantation embryo development in vitro after intracytoplasmic sperm injection. *Theriogenology* **2014**, *81*, 309–314. [\[CrossRef\]](#)
55. Jing, M.; Han, G.; Wan, J.; Zhang, S.; Yang, J.; Zong, W.; Niu, Q.; Liu, R. Catalase and superoxide dismutase response and the underlying molecular mechanism for naphthalene. *Sci. Total Environ.* **2020**, *736*, 139567. [\[CrossRef\]](#)
56. Mokhtari, K.; Perez-Jimenez, A.; Garcia-Salguero, L.; Lupiáñez, J.A.; Rufino-Palomares, E.E. Unveiling the Differential Antioxidant Activity of Maslinic Acid in Murine Melanoma Cells and in Rat Embryonic Healthy Cells Following Treatment with Hydrogen Peroxide. *Molecules* **2020**, *25*, 4020. [\[CrossRef\]](#)
57. Dong, H.; Qiang, Z.; Chai, D.; Peng, J.; Xia, Y.; Hu, R.; Jiang, H. Nrf2 inhibits ferroptosis and protects against acute lung injury due to intestinal ischemia reperfusion via regulating SLC7A11 and HO-1. *Aging* **2020**, *12*, 12943–12959. [\[CrossRef\]](#)
58. Lai, Y.L.; Lin, C.Y.; Jiang, W.C.; Ho, Y.C.; Chen, C.H.; Yet, S.F. Loss of heme oxygenase-1 accelerates mesodermal gene expressions during embryoid body development from mouse embryonic stem cells. *Redox. Biol.* **2018**, *15*, 51–61. [\[CrossRef\]](#)
59. Han, Y.; Yuan, C.; Zhou, X.; Han, Y.; He, Y.; Ouyang, J.; Zhou, W.; Wang, Z.; Wang, H.; Li, G. Anti-Inflammatory Activity of Three Triterpene from Hippophae rhamnoides L. in Lipopolysaccharide-Stimulated RAW264.7 Cells. *Int. J. Mol. Sci.* **2021**, *22*, 2009. [\[CrossRef\]](#)
60. Thouas, G.A.; Trounson, A.O.; Wolvetang, E.J.; Jones, G.M. Mitochondrial dysfunction in mouse oocytes results in preimplantation embryo arrest in vitro. *Biol. Reprod.* **2004**, *71*, 1936–1942. [\[CrossRef\]](#)
61. Wilding, M.; Dale, B.; Marino, M.; di Matteo, L.; Alviggi, C.; Pisaturo, M.L.; Lombardi, L.; De Placido, G. Mitochondrial aggregation patterns and activity in human oocytes and preimplantation embryos. *Hum. Reprod.* **2001**, *16*, 909–917. [\[CrossRef\]](#) [\[PubMed\]](#)
62. Flores-Herrera, O.; Olvera-Sanchez, S.; Esparza-Perusquia, M.; Pardo, J.P.; Rendon, J.L.; Mendoza-Hernandez, G.; Martinez, F. Membrane potential regulates mitochondrial ATP-diphosphohydrolase activity but is not involved in progesterone biosynthesis in human syncytiotrophoblast cells. *Biochim. Biophys. Acta* **2015**, *1847*, 143–152. [\[CrossRef\]](#) [\[PubMed\]](#)
63. Kohnke, D.; Ludwig, B.; Kadenbach, B. A threshold membrane potential accounts for controversial effects of fatty acids on mitochondrial oxidative phosphorylation. *FEBS Lett.* **1993**, *336*, 90–94. [\[CrossRef\]](#)
64. Treulen, F.; Uribe, P.; Boguen, R.; Villegas, J.V. Mitochondrial permeability transition increases reactive oxygen species production and induces DNA fragmentation in human spermatozoa. *Hum. Reprod.* **2015**, *30*, 767–776. [\[CrossRef\]](#) [\[PubMed\]](#)
65. Midzak, A.S.; Chen, H.; Aon, M.A.; Papadopoulos, V.; Zirkin, B.R. ATP synthesis, mitochondrial function, and steroid biosynthesis in rodent primary and tumor Leydig cells. *Biol. Reprod.* **2011**, *84*, 976–985. [\[CrossRef\]](#) [\[PubMed\]](#)
66. Odinkova, I.V.; Sung, K.F.; Mareninova, O.A.; Hermann, K.; Evtodienko, Y.; Andreyev, A.; Gukovsky, I.; Gukovskaya, A.S. Mechanisms regulating cytochrome c release in pancreatic mitochondria. *Gut* **2009**, *58*, 431–442. [\[CrossRef\]](#)
67. Wang, H.; Liu, B.; Yin, X.; Guo, L.; Jiang, W.; Bi, H.; Guo, D. Excessive zinc chloride induces murine photoreceptor cell death via reactive oxygen species and mitochondrial signaling pathway. *J. Inorg. Biochem.* **2018**, *187*, 25–32. [\[CrossRef\]](#) [\[PubMed\]](#)
68. Van Blerkom, J.; Cox, H.; Davis, P. Regulatory roles for mitochondria in the peri-implantation mouse blastocyst: Possible origins and developmental significance of differential DeltaPsi<sub>m</sub>. *Reproduction* **2006**, *131*, 961–976. [\[CrossRef\]](#) [\[PubMed\]](#)
69. Morais, R.; Guertin, D.; Kornblatt, J.A. On the contribution of the mitochondrial genome to the growth of Chinese hamster embryo cells in culture. *Can. J. Biochem.* **1982**, *60*, 290–294. [\[CrossRef\]](#)
70. Fang, J.; Uchiumi, T.; Yagi, M.; Matsumoto, S.; Amamoto, R.; Takazaki, S.; Yamaza, H.; Nonaka, K.; Kang, D. Dihydro-orotate dehydrogenase is physically associated with the respiratory complex and its loss leads to mitochondrial dysfunction. *Biosci. Rep.* **2013**, *33*, e00021. [\[CrossRef\]](#)

**Disclaimer/Publisher’s Note:** The statements, opinions and data contained in all publications are solely those of the individual author(s) and contributor(s) and not of MDPI and/or the editor(s). MDPI and/or the editor(s) disclaim responsibility for any injury to people or property resulting from any ideas, methods, instructions or products referred to in the content.